Underwater-shock compaction of hydroxyapatite-zirconia bio-composites powder

Akira Chiba[†], Yasuhiro Morizono, and Daisuke Michishita

Faculty of Engineering, Kumamoto University, 2-39-1 Kurokami, Kumamoto City, Kumamoto 860-8555, JAPAN
[†]corresponding author: chiba@gpo.kumamoto-u.ac.jp

Abstract

 Hydroxyapatite-zirconia (HAp-ZrO_2) bio-composites were fabricated by our newly developed underwater-shock compaction technique. Hydroxyapatite [HAp; $Ca_{10}(PO_4)(OH)_2$] is well known to be a bioactive ceramic having excellent biocompatibility with body environment. However, fracture strength and toughness of this bio-ceramic itself are low and its tensile strength does not withstand to practical use for implant materials.

 Therefore, ZrO_2 powder is added to HAp powder in order to obtain good mechanical properties of HAp without any degradation of biocompatibility,.

 Experimental assembly for underwater-shock compaction consists of three parts, i.e. explosive container, water tank and powder container from top to bottom. The water tank is shaped to be a circular cone, and so, the energy of shock wave was increased by the convergence of shock wave due to the reduction of cross section area of the water tank. Sound compacts of HAp-ZrO_2 composites without any cracks and tears were fabricated. The relative densities of the composites were more than 80 % as compared with 40 % stacking density. The compacts were post-sintered at various temperatures. The structures were almost the same as the as-compacted state to 1373 K sintering. Fracture toughness was obtained to be 3.04 MPa $\sqrt{m}$, which is equal to that of human bone. As a result, the addition of ZrO_2 is confirmed to be effective for an improvement of low fracture strength of HAp.

Keywords: Shock compaction, Hydroxyapatite, Zirconia, Bio-composites, Powder compaction

1. Introduction

 Hydroxyapatite(HAp) exhibits excellent biocompatibility in the human body and therefore is one of the most widely used bioactive ceramics for artificial tooth and bone. However, since fracture strength and toughness of this ceramics are low, it cannot endure practical use [1]–[6].

 Therefore, zirconia powder is added to HAp powder in order to obtain high fracture toughness. ZrO_2 has good properties as compared with HAp, and exhibits extremely high stability with human tissues[7]–[9]. The limited stability of HAp at high temperatures during sintering should be considered since HAp will dissociate into tricalcium phosphate. On the other hand, high temperatures and long sintering duration required for consolidation of HAp powders often result in extreme grain coarsening or surface contamination, which can degrade the desired mechanical properties.

 The advantage of powder compaction utilizing underwater-shock pressure generated by the detonation of explo-sives lies in the ability to fabricate denser compacts within microseconds and without any additives such as binders[10]–[12]. Further, this explosive compaction induces localized heating only at particle surfaces, thus minimizing deleterious interactions between various powders. The purpose of the present study is to produce HAp/ZrO_2 composites by means of the underwater-shock compaction technique and to investigate the effect of addition of ZrO_2.

2. Experimental procedure
2.1 Materials

 HAp powder and ZrO_2 powder containing 3 mol % yttrium were provided by Taihei chemical industry Co., Ltd. and Toso industry, Co., Ltd, respectively. HAp powder was formed as an aggregate of primary particles of about 0.2~0.3 μm, and the ZrO_2 powder was formed as an aggregate of primary particles of about 0.3 μm. HAp powder had a Ca/Ti ratio of 1.67. HAp/ ZrO_2 mixed powders by
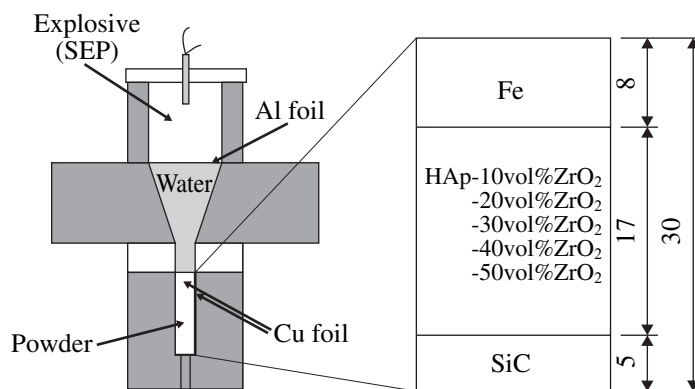
Fig. 1 Schematic illustrations of underwater-shock compaction assembly and powder stacking (unit: mm).

changing the volume percent of HAp: ZrO_2 from 90:10 to 50:50 were prepared by the wet milling with ethanol for 86.4 ks (24 h) at room temperature.

2.2 Milling conditions of powders and assembly for underwater shock compaction

The hydroxyapatite powder and zirconia powder were milled in a ceramic bottle with zirconia balls for 86.4 ks. The milling medium was ethyl alcohol. The mixed powder was used for explosive compaction.

As shown in Fig. 1, experimental assembly for underwater-shock compaction consists of three parts, i.e. explosive container, water tank and powder container from top to bottom. The feature of this assembly is that water is used as pressure medium. The water tank is shaped to be a circular cone, and so, the energy of shock wave was increased by the convergence of shock wave due to the reduction of cross section area of the water tank. The shock pressure and duration time are easily controlled by changing the type and weight of explosives.

The compaction process is as follows. The shock wave produced by the detonation of explosive travels from the top to bottom of the water tank. The water tank is machined into a truncated cone so that, high pressure can be preserved by reflection and converging of shock wave and propagates into the specimen powder charging part. This high shock pressure compacts the powders in high density.

The explosive used in present study was plastic explosive SEP consisting mainly of nitric ester produced by Asahi Kasei Company. The detonation velocity of the explosive is about 6900 m/s. The shock pressure obtained by this assembly is estimated to be about 2 GPa. Fe powder and SiC powder are put at the top and bottom of the specimen powder charging part to prevent the scattering of specimen powder by shock wave and momentum trap respectively.

2.3 Characterization of structure and mechanical tests

The specimens were examined by optical microscopy and scanning electron microscopy. The crystal phases were identified using X-ray diffraction. The relative density was measured by Archimedes method. Vickers hardness and fracture toughness (K_{1c}) were measured. Fracture toughness was measured by the indentation fracture (IF) method. By this method, K_{1c} values can be calculated from hardness and length of crack that is made in corner of lozenge-shaped hollow.

3. Experimental results
3.1 Optimum compaction condition and microstructure of the compact

Figure 2 shows the external view of the compact and cross-sectional view. The height of the powder as stacked condition is 17 mm and after compaction, the height reduces to 6 mm that is 65 % of the starting height. Internal defects like cracks or tears were not found in cross-sectional area. Controlling the shock pressure, 5 kinds of specimen with changing ZrO_2 content showed good compaction states.
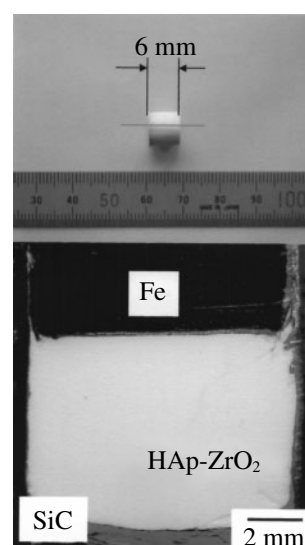
Figure 3 shows relationship between the amount of explo-

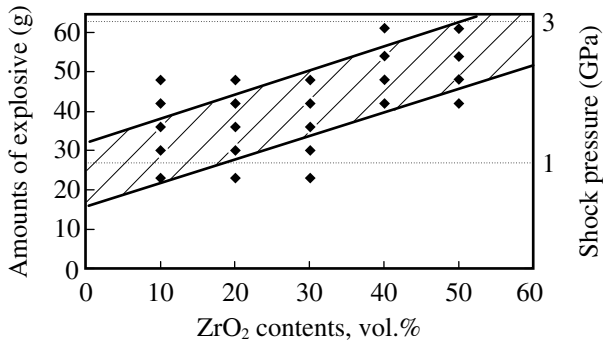Fig. 2 External view and optical micrograph of HAp-ZrO_2 compact.

Fig. 3 Relationship between the amount of explosive to get sound compacts and ZrO₂ contents.

Fig. 4 XRD patterns of the specimens before (a) and after the shock compaction (b).

sive to get sound compacts and ZO₂. The hatched region shows the region of optimum compaction gained. Increasing the zirconia content in mixed powder, the amount of explosive to gain good compact increases.

To understand the effect of shock pressure for crystal structure for the compacts, XRD patterns were investigated to the specimens before and after the shock compaction shown in Fig. 4. The specimen after compaction is constructed with HAp and the ZrO₂ of mainly tetragonal and a small amount of monoclinic structure. There is no change in XRD structure before and after the shock compaction. The boundary between the composite powders is estimated to be heated instantly above 1473 K during explosive compaction, but actually the heat generated is instantly cooled by the water chamber of this assembly.

3.2 Mechanical properties of the as-compacted samples

Figure 5 shows the hardness change for five kinds of specimens. The hardness increases with increasing ZrO₂ contents. The hardness of fully densed HAp compacts is known to be 700 Hv. The hardness obtained in this study shows lower values and is known to be week bonding between the powders. To get good bonding, the sintering treatment is known to be needed after the compaction.

The relative densities as-compacted states were between 80 to 85 % for five specimens.

Figure 6 shows the fracture toughness for five specimens. The fracture toughness increases increasing ZrO₂ content in the composites but the values are too low for practical use for implant materials.

3.3 Effects of sintering treatment for improvement of mechanical characteristics

Figure 7 shows relative densities of HAp/ZrO₂ composites of as-compacted and after sintering conditions. The relative density in as-compacted state was about 82 %. Increasing the sintering temperatures increases relative densities of the specimens. Average relative densities after sintering shows about 90 %. It is reported that 90 % relative density is good for bone permeating to HAp/ ZrO₂
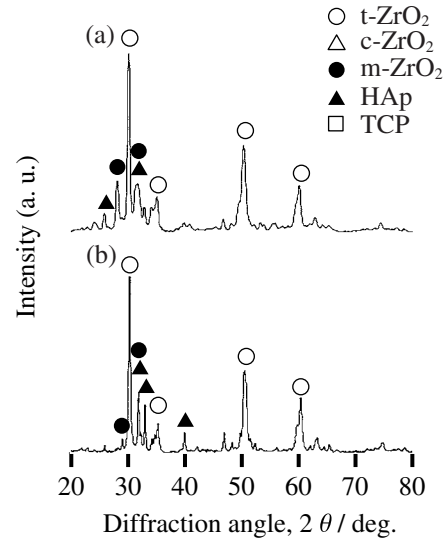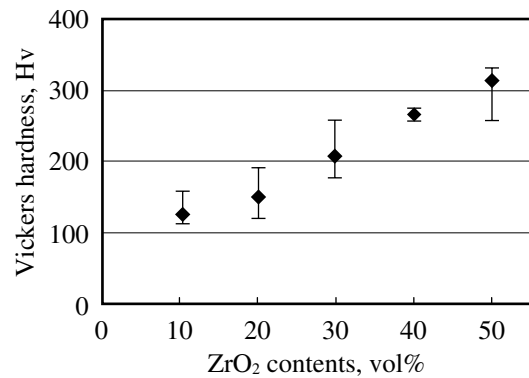

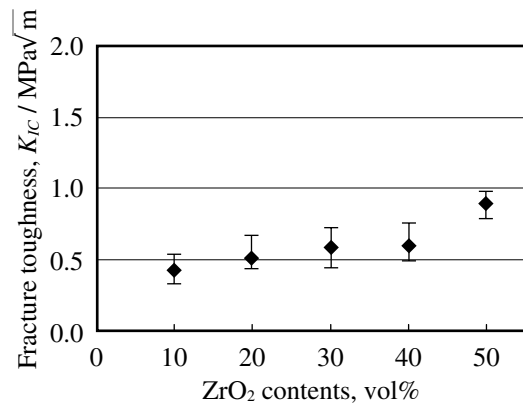Fig. 5 Vickers hardness of as-compacted specimens with various ZrO₂ contents.

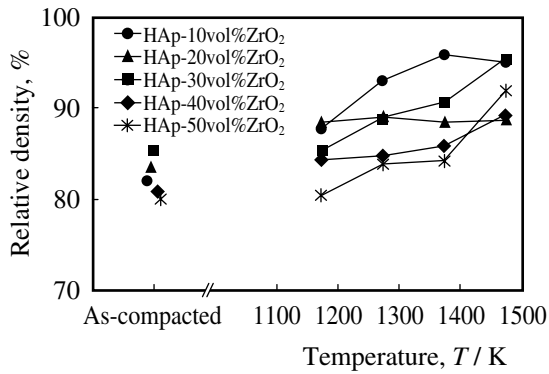Fig. 6 Fracture toughness of as-compacted specimens with various ZrO₂ contents.

Fig. 7   Relative density of HAp-ZrO$_2$ composites with as-compacted state and sintering various temperatures.
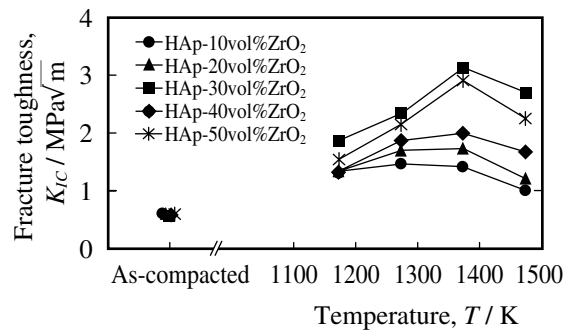

Fig. 8   Fracture toughness of HAp-ZrO$_2$ composites with as-compacted state and sintering various temperatures.

composites.

The structures are almost the same as the compacted state to 1373 K sintering by optical microscopy.

Figure 8 shows the fracture toughness of HAP/ZrO$_2$ composites sintering temperature to 1373 K by indentation fracture method. the K_{1c} values increases increasing the sintering temperature, like the hardness change for the specimens. The K_{1c} values are 0.61 MPa $\sqrt{m}$ for the specimen of as-compacted condition and 3.04 MPa $\sqrt{m}$ for the specimen sintered at 1373 K. This value is 5 times of the specimen of as-compacted condition and is equal to the value of dense human bone. As the K_{1c} value of HAp compact itself is about 1.1 MPa $\sqrt{m}$, the addition of ZrO$_2$ to HAp contributes the improvement of K_{1c} value. The K_{1c} value of specimen annealed at 1473 K decreases drastically. This is due to decomposition reaction of HAp at high temperature.
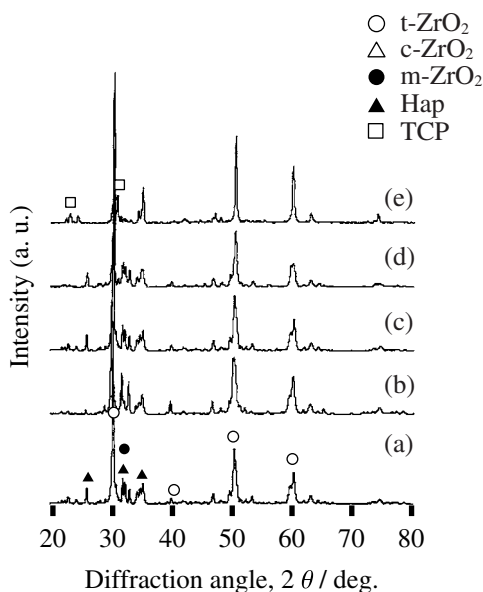

Fig. 9   XRD patterns of HAp-20 vol % ZrO$_2$ composite of (a) as-compact state and sintered states at (b) 1173 K, (c) 1273 K, (d) 1373 K, and (e) 1473 K for 14.4 ks.

3.4 Decomposition behavior of HAp during sintering

Figure 9 shows XRD analyses for as-compacted condition and sintered at various temperatures, that is (a) shows as-compacted state, (b) shows sintered at 1173 K, (c) is 1273 K sintering, (d) is 1373 K and (e) is 1473 K sintering. Samples of as-compacted state and sintering states till 1373 K show the same patterns with ZrO$_2$ and HAp but sample annealed at 1473 K shows tri-calcium phosphate (TCP) peaks due to the decomposition of HAp. TCP compounds are known to take two types, that is β-type for low temperature region and α-type for high temperature region and transition temperature is about 1473 K. The β-type phase is recognized from XRD analysis.

4. Conclusions

HAp-ZrO$_2$ bio-composites were fabricated by our newly developed underwater-shock compaction technique.

In order to obtain good mechanical properties of HAp without any degradation of biocompatibility, ZrO$_2$ was added to HAp powder. The results obtained are as follows;

(1) Experimental assembly for underwater-shock compaction consists of three parts, i.e. explosive container, water tank and powder container from top to bottom. The water tank is shaped to be a circular cone, and so, the energy of shock wave was increased by the convergence of shock wave due to the reduction of cross section area of the water tank. The explosive used consists mainly of nitric ester. Its detonation speed is about 6900 m/s.

(2) Sound compacts of HAp-ZrO$_2$ composites without any cracks and tears were fabricated. The relative densities of the composites were more than 80 % as compared with 40 % stacking density.

(3) The compacts were post-sintered at various temperatures. The structures were almost the same as the as-compacted state to 1373 K sintering. However, when the compacts were sintered at 1473 K, tri-calcium phosphate was identified by X-ray analysis by decomposition of HAp. The optimum sintering temperature was 1373 K.

(4) Fracture toughness was obtained to be 3.04 MPa $\sqrt{m}$, which is equal to that of human bone.

References

1) M. Akao, H. Aoki, K. Kato, J. Mater. Sci., 16, 809 (1981).
2) H. M. Kim, J. Ceram. Jpn., 199, S49 (2001).
3) A. Krajewski, A. Ravaglioli, L. Riva di Sanseverin, F. Marchetti, G. Monticelli, Biomaterials, 5, 105 (1981).
4) J. Zhou, X. Zhang, J. Chen, S. Zeng, K.D.E. Groot, J. Mater. Sci. Mater. Med., 4, 83 (1993).
5) D. S. Metsger, M. R. Rieger, D. W. Foreman, J. Mater. Sci. Mater. Med., 10, 9 (1999).
6) G. Dewith, H. J. A. Vandijk, N. Hattu, K. Prijs., J. Mater. Sci. 16, 1592 (1981).
7) J-M Wu, T-S Yeh, J. Mat. Sci., 23, 3771 (1988).
8) M. Takagi, M. Mochida, N. Uchida, K. Saito, K. Uematsu, J. Mater. Sci. Mater. Med., 3, 199 (1992).
9) Y. W. Gu, N. H. Loh, K. A. Khor, S. B. Tor, P. Cheang, Biomaterials, 23, 37 (2002).
10) A. Chiba, M. Fujita, M. Nishida, K. Imamura, R. Tomoshige, "Shock-Wave and High-Strain-Rate Phenomena in Materials", 415 (1992) Marcel Dekker.
11) A. Chiba, M. Nishida, K. Imamura, Y. Morizono, S. Itoh, M. Fujita, "Shock Waves", Panther, Fyshwick, Australia, 1225 (1998).
12) H. Matsumoto, K. Kondo, A. Sawaoka, J. Jpn. Inst. Metals 52, 810 (1988).

ハイドロキシアパタイト-ジルコニア系 生体複合粉末の水中衝撃圧縮

千葉 昂[†]，森園靖浩，道下大輔

　ハイドロキシアパタイト-ジルコニア系生体複合粉末を用いて水中衝撃圧縮を試みた。

　優れた生態適合性を示すハイドロキシアパタイトは，人工歯根や人工骨などの生体用インプラント材として実用化が期待されるセラミックスである。しかしながら，このセラミックスは破壊強度及び破壊靱性などの機械的特性が乏しいため，その利用範囲は限られている。そこで本研究ではこのセラミックスの強靱化を図るため，機械的強度が優れ，かつ生体親和性に優れるジルコニア粉末を添加することによって，良好な機械的性質を得ることを目的とした。水中衝撃圧縮法のための実験装置は爆薬充填部，水槽部及び粉末充填部の3層から構成されている。水槽部は円錐状に成型し，衝撃エネルギーは下部に行くにつれ，水槽断面積が減少することにより，衝撃波の反射，収束により，増加させている。この方法により，焼結助剤を用いることなく，割れ等の欠陥のない良好なハイドロキシアパタイト-ジルコニア系生体複合体を作製できた。この複合材の相対密度は充填時の40％から圧縮後80％以上が得られた。この複合体は種々の温度で焼結を行った。組織は1373 Kまでは圧縮ままとほぼ同一であった。破壊靱性は $3.04\,\mathrm{MPa}\sqrt{\mathrm{m}}$ とほぼ人骨の値に等しい値が得られた。この結果より，ハイドロキシアパタイトの強化に対し，ジルコニア粉末添加が有効であることを見出した。

熊本大学工学部　〒860-8555　熊本市黒髪2-39-1
[†] corresponding author: chiba@gpo.kumamoto-u.ac.jp